Dynamics of lump chains for the BKP equation describing propagation of nonlinear waves

Zhonglong Zhao(赵忠龙)[1,†], Lingchao He(和玲超)[2], and Abdul-Majid Wazwaz[3]

[1] *School of Mathematics, North University of China, Taiyuan* 030051, *China*
[2] *College of Mathematics, Taiyuan University of Technology, Taiyuan* 030024, *China*
[3] *Department of Mathematics, Saint Xavier University, Chicago, IL* 60655, *USA*

(Received 28 November 2022; revised manuscript received 30 December 2022; accepted manuscript online 6 January 2023)

A large member of lump chain solutions of the $(2+1)$-dimensional Bogoyavlenskii–Kadomtsev–Petviashvili (BKP) equation are constructed by means of the τ-function in the form of Grammian. The lump chains are formed by periodic arrangement of individual lumps and travel with distinct group and velocities. An analytical method related dominant regions of polygon is developed to analyze the interaction dynamics of the multiple lump chains. The degenerate structures of parallel, superimposed, and molecular lump chains are presented. The interaction solutions between lump chains and kink-solitons are investigated, where the kink-solitons lie on the boundaries of dominant region determined by the constant term in the τ-function. Furthermore, the hybrid solutions consisting of lump chains and individual lumps controlled by the parameter with high rank and depth are investigated. The analytical method presented in this paper can be further extended to other integrable systems to explore complex wave structures.

Keywords: lump chains, interaction solutions, BKP equation

PACS: 05.45.Yv, 02.30.Jr, 02.30.Ik **DOI:** 10.1088/1674-1056/acb0c1

1. Introduction

An important characteristic of integrable systems is that they possess localized wave solutions that are of physical interest. The lump wave is a remarkable localized wave solution degenerating in the whole space.[1–7] The lump solution is actually a kind of rational solutions from a mathematical point of view, whose simplest form was first discovered by means of the dressing method and the Hirota's bilinear method.[8–10] This solution consists of multiple localized peaks remaining their velocities and trajectories unchanged before and after the interactions. However, some high-order lumps with same velocities undergo anomalous scattering, which may form the bound states of the lumps called multi-lumps.[11,12] The research indicates that either simple and multi-lump solutions of the Kadomtsev–Petviashvili I (KPI) equation are rational potentials associated with the Schrödinger equation. It is also interesting that the dynamics of the KPI lumps have a close connection with the multi-particle Calogero–Moser system.[13,14] A large family of rational multi-lump solutions of the KPI equation were obtained by means of the Gramian method by Chakravarty and Zowada. They proved that there exists a one-to-one correspondence between the multi-lump solutions and partitions of a positive integer N.[15,16] A reduced version of the Grammian form solution was employed to present a direct method to study the multi-lump molecules of the KPI equation.[17] A new type of lump molecules appearing in a period of time of the KPI equation was obtained.[18] The pattern transformation in high-order lumps of the KPI equation was investigated, which shows two types of solution patterns appear at large time. The arrangement structure of the lumps are related to the nonzero-roots of the Wronskain–Hermit and Yablonskii–Vorob'ev polynomials.[19]

In addition to the study of multi-lump solutions of the integrable systems, the interaction solutions between lump waves and other localized waves including solitons, breathers, and resonant solitons have attracted more and more scholars' attention. The partial long wave limit method is a most effective method to study the interactions between multi-lumps and solitons, especially the resonant solitons.[20–22] By combining the reduction method for the KP hierarchy and Hirota bilinear technique, a general interaction solution between L-lump and $L+1$-line-solitons of the KPI equation was constructed.[23] The lumps are initially released by some solitons and then absorbed by remaining solitons. A similar interaction between $n(n+1)/2$ solitonic lumps and multi-solitons in a intermediate time was investigated by Guo *et al.* through binary Darboux transformation.[24] Rao *et al.* studied partial and complete resonant collisions of lumps and homoclinic orbits for the two-dimensional multi-component long-wave-short-wave resonance interaction system.[25] The resonant collision solutions between lumps and dark solitons called lump-typed rogue waves were derived.[26] The elastic interactions between lumps and solitons on the periodic background to the nonlo-

†Corresponding author. E-mail: zhaozlhit@163.com, zhaozl@nuc.edu.cn
© 2023 Chinese Physical Society and IOP Publishing Ltd

cal Mel'nikov equation were investigated.[27] From the perspective of solution in form of Grammian, Stepanyants *et al.* systematically studied the interactions among lumps, solitons, and lump chains of the KPI equation. The lumps and periodic lump chains can be absorbed and emitted by the line solitons.[28] A broad class of lump chains of the KPI equation were obtained by using a reduced version of τ-function in the form of Grammian.[29] The lump chain of the KP equation is already known, which is also called the breather and periodic soliton.[30,31] The lump chains are formed by periodic arrangement of individual lumps and travel with distinct group and velocities. The interaction between the lump chains can be regarded as the phenomenon of resonance of the breathers.[32,33] A new kind of interaction solutions consisting of two weakly interacting lump waves and line waves for the KPI equation was presented by means of some clever limit tricks.[34] The anomalous interactions of multilumps and some kinds of bound states of lumps of the KPI equation were studied via M-lump solutions in the form of the determinant.[35]

The $(2+1)$-dimensional Bogoyavlenskii–Kadomtsev–Petviashvili (BKP) equation

$$u_{xxt}+u_{xxxxy}+12u_{xx}u_{xy}+8u_xu_{xxy}+4u_{xxx}u_y=u_{yyy}, \tag{1}$$

is a modification of Calogero–Bogoyavlenskii–Schif equation,[36,37] which can be extended to describe propagation dynamics of nonlinear waves appearing in physics, biology, and electrical networks.[38] The BKP equation is integrable in sense of Painlevé property and Lax representation.[39] Various new solutions including soliton-like, period, and rational solutions of Eq. (1) were obtained.[40] The nonlocal symmetry, Bäcklund transformation, and CRE solvability of the BKP equation were studied systematically.[41] A kind of high-order lump waves and rogue waves of the BKP equation was given in Ref. [42], which indicates this equation has the complex wave structure. Various interaction solutions among the lumps, lump molecules, solitons, and lump chains of the BKP equation were studied via the solutions in the form of Grammian. The breathers of the BKP equation and some patterns had been investigated by Yuan *et al.*[43] An analytical method related to dominant domains was developed to analyze the interaction dynamical behaviors of the hybrid solutions.[44] Inspired by works,[28,29] the lump chains and interaction dynamics of the BKP equation will be investigated systematically.

The organization of the paper is as follows. In Section 2, the solution in the form of Grammian of the BKP equation is briefly introduced. In Section 3, a large family of lump chains of depth $P=0$ are constructed. An analytical method related dominant regions of polygon is developed to analyze the interaction dynamics of the multiple lump chains. Some degenerate cases of the lump chains are discussed to enrich the type of the solutions. Section 4 focus on investigating the interaction solutions between lump chains and kink-solitons. In Section 5, the hybrid solutions consisting of individual lumps and lump chains controlled by the parameter s are constructed, which can be regard as a new type of rogue wave solutions. Finally, some conclusions and discussions are given in the last section.

2. The τ-function in the form of Grammian

Based on the bilinear theory, equation (1) can be transformed into the following bilinear equations:

$$\begin{aligned}&\left(D_x^4-3D_xD_s-3D_y^2\right)\tau\cdot\tau=0,\\&\left(3D_xD_t+2D_x^3D_y+3D_yD_s\right)\tau\cdot\tau=0,\end{aligned}$$

by means of the variable transformation

$$u=(\ln\tau)_x=\frac{\tau_x}{\tau}, \tag{2}$$

where $\tau(x,y,t,s)$ is a solution of above bilinear system, x and y are spatial variables, t is a time variable and the s is the auxiliary independent variable, and the Hirota's bilinear operators are defined by[45–47]

$$D_x^{N_1}D_y^{N_2}D_t^{N_3}D_s^{N_4}(\tau\cdot g)=(\partial_x-\partial_{x'})^{N_1}\left(\partial_y-\partial_{y'}\right)^{N_2}(\partial_t-\partial_{t'})^{N_3}(\partial_s-\partial_{s'})^{N_4}\tau(x,y,t,s)\,g\left(x',y',t',s'\right)\big|_{x'=x,y'=y,t'=t,s'=s}.$$

The purpose of this paper is to investigate a series of solutions of the BKP Eq. (1) by using the Grammian form of the τ-function. Through the formula of Wronskian, the BKP equation has the solution in the form of Grammian[48]

$$\begin{aligned}&u(x,y,t,s)=(\ln\tau(x,y,t,s))_x,\\&\tau(x,y,t,s)=\det\left[c_{jk}+\int_{-\infty}^{x}\varphi_j\left(x',y,t,s\right)\overline{\varphi}_k\left(x',y,t,s\right)\mathrm{d}x'\right],\end{aligned} \tag{3}$$

where $\varphi(x,y,t,s)$ is a linearly independent set of solutions of the linear system

$$\varphi_t=2\mathrm{i}\varphi_{xxxx},\quad \varphi_y=-\mathrm{i}\varphi_{xx},\quad \varphi_s=\frac{4}{3}\varphi_{xxx}, \tag{4}$$

and $\overline{\varphi}$ satisfies the conjugate system

$$\overline{\varphi}_t=-2\mathrm{i}\overline{\varphi}_{xxxx},\quad \overline{\varphi}_y=\mathrm{i}\overline{\varphi}_{xx},\quad \overline{\varphi}_s=\frac{4}{3}\overline{\varphi}_{xxx}. \tag{5}$$

To consider the function $\varphi_j(x,y,t,s)$ with finite spectral sup-

port, the function possessing the eigenvalues λ with positive real parts is introduced as follows:

$$\sigma(x,y,t,s,\lambda)=\lambda x-\mathrm{i}\lambda^2 y+2\mathrm{i}\lambda^4 t+\frac{4}{3}\lambda^3 s. \tag{6}$$

More generally, the homogeneous polynomial of degree p is given as

$$\rho_p(x,y,t,s,\lambda)=\mathrm{e}^{-\sigma(x,y,t,s,\lambda)}\frac{\partial^p}{\partial\lambda^p}\mathrm{e}^{\sigma(x,y,t,s,\lambda)}. \tag{7}$$

Utilizing this formula, a series of polynomial functions are obtained as follows:

$$\begin{aligned}&\rho_0=1,\\&\rho_1=x-2\mathrm{i}\lambda y+8\mathrm{i}\lambda^3 t+4\lambda^2 s,\\&\rho_2=\left(x-2\mathrm{i}\lambda y+8\mathrm{i}\lambda^3 t+4\lambda^2 s\right)^2+\left(-2\mathrm{i}y+24\mathrm{i}\lambda^2 t+8\lambda s\right),\\&\cdots.\end{aligned}$$

It is easy to prove that $\partial_\lambda^p\,\mathrm{e}^{\sigma(x,y,t,s)}=\rho_\mathrm{p}\,\mathrm{e}^{\sigma(x,y,t,s)}$ is a solution of the linear system (4) for any value of λ. For constructing a member of the solutions in terms of τ-function (3), the eigenfunctions $\varphi_j(x,y,t,s)$ can be given by

$$\varphi_j(x,y,t,s)=\sum_{n=1}^{N}\sum_{p=0}^{P}C_{jnp}\rho_\mathrm{p}(x,y,t,s,\lambda_{jn})\,\mathrm{e}^{\sigma(x,y,t,s,\lambda_{jn})}, \tag{8}$$

where the positive integer N is called the order of the solution, the highest degree P of a polynomial ρ_p is called the depth of the solution, λ_{jn} are eigenvalues and the coefficient C_{jnp} is required to make the functions $\varphi_j(x,y,t,s)$ linearly independent.

3. Lump chains of depth $P=0$

In this section, we consider the solutions of the BKP Eq. (1) possessing the structure of lump chains. For the first case, we consider the reduced case $c_{jk}=0$ and the eigenfunction $\varphi_j(x,y,t,s)$ is determined by formula (8) with depth $P=0$. Let the rank of the solution $M=1$, then the solution (3) in the form of Grammian can be reduced to

$$\begin{aligned}&u(x,y,t,s)=(\ln\tau(x,y,t,s))_x,\\&\tau(x,y,t,s)=\int_{-\infty}^{x}\left|\varphi(x',y,t,s)\right|\mathrm{d}x',\end{aligned} \tag{9}$$

where the function $\varphi(x',y,s,t)$ is a sum of $N\geq 2$ exponentials as shown in formula (8). The solution (9) is arranged in a chain by lumps, in which every lump travels along the chain with a constant velocity and all the lumps as a whole evolves with time t. The spatial structure and evolutionary behavior of this lump chain are similar to the well-known line-soliton of the KP II equation.[49] To write the solution (9) into a more clear expression, the following restrictive condition is introduced

$$\lambda_n=\alpha_n+\mathrm{i}\beta_n,\qquad \eta_n=k_n+\mathrm{i}l_n,$$

where $\alpha_n>0$ and $\lambda_n\neq\lambda_m\,(n\neq m)$. A polynomial function with the eigenvalue λ_n is given as

$$\Psi_n(x,y,t,s)=\lambda_n x-\mathrm{i}\lambda_n^2 y+2\mathrm{i}\lambda_n^4 t+\frac{4}{3}\lambda_n^3 s+\eta_n,$$

then the function

$$\varphi(x,y,t,s)=\sum_{n=1}^{N}\sqrt{2\alpha_n}\,\mathrm{e}^{\Psi_n(x,y,t,s)} \tag{10}$$

satisfies the linear equations (4). Substituting Eq. (10) into Eq. (9), the τ-function in the solution (9) can be expanded as

$$\tau(x,y,t,s)=\sum_{n=1}^{N}\mathrm{e}^{2F_n}+\sum_{n=1}^{N-1}\sum_{m=n+1}^{N}4\theta_{nm}\,\mathrm{e}^{F_n+F_m}\cos(G_n-G_m-\delta_{nm}), \tag{11}$$

where the function F_n and G_n are determined by

$$\begin{aligned}&F_n(x,y,s,t)=\mathrm{Re}\Psi_n(x,y,s,t)=\alpha_n x+2\alpha_n\beta_n y+\left(8\alpha_n\beta_n^3-8\alpha_n^3\beta_n\right)t+\left(\frac{4}{3}\alpha_n^3-4\alpha_n\beta_n^2\right)s+k_n,\\&G_n(x,y,s,t)=\mathrm{Im}\Psi_n(x,y,s,t)=\beta_n x+\left(\beta_n^2-\alpha_n^2\right)y+\left(2\beta_n^4+2\alpha_n^4-12\alpha_n^2\beta_n^2\right)t+\left(4\alpha_n^2\beta_n-\frac{4}{3}\beta_n^3\right)s+l_n,\end{aligned}$$

and the coefficients θ_{nm} and δ_{nm} are given by

$$\begin{aligned}&\theta_{nm}=\sqrt{\frac{\alpha_n\alpha_m}{(\alpha_n+\alpha_m)^2+(\beta_n-\beta_m)^2}},\\&\delta_{nm}=\arctan\left(\frac{\beta_n-\beta_m}{\alpha_n+\alpha_m}\right).\end{aligned}$$

The large-scale structure of solution (9) is determined by the relative values of the linear function $F_n(x,y,t,s)$. For a fixed time t and parameter s, we consider the following sets:

$$\Delta_n=\Delta_n(t,s)=\left\{(x,y)\in R^2:F_n(x,y,t,s)\geq F_m(x,y,t,s)\right\}, \tag{12}$$

where $m\neq n$ and $n=1,2,\ldots,N$. The (x,y)-plane is divided into finitely polygons by the regions $\Delta_1(t,s),\ldots,\Delta_N(t,s)$. The partition evolves linearly with time t and auxiliary variable s, when one of t and s is a fixed value. Based on the theory of ele-

mentary linear algebra, for a point (x,y) in the region $\Delta_n(t,s_0)$ located at a distance l to the boundary, *i.e.*, the distance to the other region $\Delta_m(t,s_0)$ is at least l, then there exists a constant $c>0$ to make the following conclusion tenable:

$$F_n(x,y,t,s_0)-F_m(x,y,t,s_0)\geq cl.$$

This fact indicates that the exponential term $\mathrm{e}^{2F_n(x,y,t,s_0)}$ in the τ-function (11) is dominant when the point near the above point (x,y), *i.e.*,

$$\tau(x,y,t,s_0)=\mathrm{e}^{2F_n}(1+h(x,y,t,s_0)),\qquad |h|<C\mathrm{e}^{-cl}.$$

Since the term e^{2F_n} can be eliminated when taking the first logarithmic derivative, therefore the solution $u(x,y,t,s_0)$ is exponentially small near (x,y). Based on the above analyses, the solution (9) having the τ-function (11) is exponentially small in the interiors of the Δ_n. What is more, the solution (9) has the spatial structure of gathering on a narrow strips along the boundaries where two of the Δ_n intersect.

3.1. Lump chains with $M=1$ and $N=2$

If we choose $M=1$ and $N=2$ in the solution of lump chain (9), the single lump chain solution can be obtained as

$$u(x,y,t,s)=\frac{\partial}{\partial x}\ln\left[\cosh(F_1-F_2)+2\theta_{12}\cos(G_1-G_2-\delta_{12})\right]. \tag{13}$$

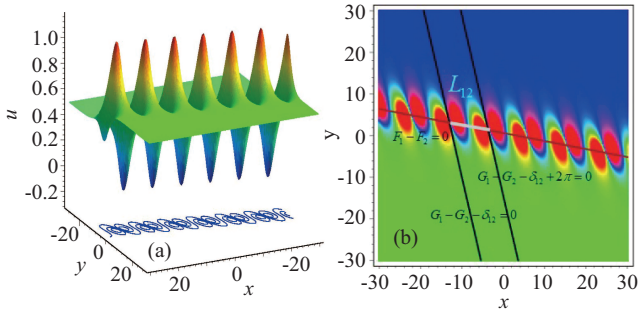


Fig. 1. The single lump chain (9) with the eigenvalues $\lambda_1=1/3+\mathrm{i}/2$ and $\lambda_2=1/4-\mathrm{i}/5$. (a) The lump chain $u(x,y,t=0,s=1)$, (b) the density map and characteristic lines of lump chain.

Figure 1(a) is plotted to show the spatial structure of the lump chain, which is a linear traveling wave consisting of infinite number of lump waves. The regions are separated by the line $F_1-F_2=0$ and the plane (x,y) is divided into two half-planes, which can be observed in Fig. 1(b). Solution (13) is supported on a narrow strip along the line $F_1-F_2=0$, which reflects the locality of the lump chain. As shown in Fig. 1(b), the lump waves are periodically arranged along the straight line $F_1-F_2=0$, meanwhile the line $G_1-G_2-\delta_{12}=0$ determines the rotation direction of the lump wave. We mark the above two lines as two characteristic lines of the lump chain $(L_1: F_1-F_2=0; L_2: G_1-G_2-\delta_{12}=0)$. By analyzing the direction of characteristic line L_1, one obtains that

$$\boldsymbol{U}_{12}=(\alpha_1-\alpha_2,2\alpha_1\beta_1-2\alpha_2\beta_2)$$

is a direction vector of the lump chain. In particular, the lump chain can be reduced to the "Akhmediev" and "Kuznetsov–Ma" breathers[50–52] as $\alpha_1-\alpha_2=0$ and $2\alpha_1\beta_1-2\alpha_2\beta_2=0$, respectively. In order to further analyze the dynamic characteristics of the lump chain, the following notation is introduced:

$$\begin{aligned}
&F_n-F_m=A_{nm}x+B_{nm}y+C_{nm}t+D_{nm}s+E_{nm},\\
&G_n-G_m-\delta_{nm}=\tilde{A}_{nm}x+\tilde{B}_{nm}y+\tilde{C}_{nm}t+\tilde{D}_{nm}s+\tilde{E}_{nm},\\
&A_{nm}=\alpha_n-\alpha_m,\ B_{nm}=2(\alpha_n\beta_n-\alpha_m\beta_m),\\
&C_{nm}=8(\alpha_n\beta_n^3-\alpha_m\beta_m^3)-8(\alpha_n^3\beta_n-\alpha_m^3\beta_m),\\
&\tilde{A}_{nm}=\beta_n-\beta_m,\ \tilde{B}_{nm}=\beta_n^2-\beta_m^2-(\alpha_n^2-\alpha_m^2),\\
&\tilde{C}_{nm}=(2\beta_n^4+2\alpha_n^4-12\alpha_n^2\beta_n^2)-(2\beta_m^4+2\alpha_m^4-12\alpha_m^2\beta_m^2),
\end{aligned}$$

where the phases $D_{nm}s+E_{nm}$ and $\tilde{D}_{nm}s+\tilde{E}_{nm}$ play an auxiliary to analyze the lump chain, thus it is not necessary to write out the displayed formula. The lump chain consists of a sequence of lumps and each lump propagates with velocity vector (V_x,V_y)

$$\begin{aligned}
V_x&=\frac{B_{12}\tilde{C}_{12}-C_{12}\tilde{B}_{12}}{A_{12}\tilde{B}_{12}-B_{12}\tilde{A}_{12}}=\frac{4\left(\alpha_1{}^2+2\alpha_1\alpha_2+\alpha_2{}^2+(\beta_1+\beta_2)^2\right)(\alpha_1\beta_1+\alpha_2\beta_2)}{\alpha_1+\alpha_2},\\
V_y&=\frac{C_{12}\tilde{A}_{12}-A_{12}\tilde{C}_{12}}{A_{12}\tilde{B}_{12}-B_{12}\tilde{A}_{12}}=\frac{-6\left[-\frac{1}{3}\alpha_1{}^3-\frac{1}{3}\alpha_2\alpha_1{}^2+\left(\frac{1}{3}\beta_2{}^2+\frac{2}{3}\beta_2\beta_1-\frac{1}{3}\alpha_2{}^2+\beta_1{}^2\right)\alpha_1+\frac{1}{3}\alpha_2\left(3\beta_2{}^2+2\beta_2\beta_1-\alpha_2{}^2+\beta_1{}^2\right)\right]}{\alpha_1+\alpha_2}.
\end{aligned}$$

If we regard the lump chain as a whole and ignore the periodic motion of a single lump, the overall speed of the lump chain is

$$\boldsymbol{V}_{12}=\frac{-C_{12}}{A_{12}^2+B_{12}^2}(A_{12},B_{12}).$$

By analyzing two parallel characteristic lines in Fig. 1(b), the distance between two consecutive lumps has the expression

$$L_{12}=\frac{2\pi\sqrt{A_{12}^2+B_{12}^2}}{|A_{12}\tilde{B}_{12}-B_{12}\tilde{A}_{12}|}=\frac{2\pi\sqrt{\left(4\beta_1{}^2+1\right)\alpha_1{}^2+(-8\beta_2\beta_1-2)\alpha_2\alpha_1+\alpha_2{}^2\left(4\beta_2{}^2+1\right)}}{(\alpha_1+\alpha_2)\left((\alpha_1-\alpha_2)^2+(\beta_1-\beta_2)^2\right)}.$$

Thus we can conclude that the period of the lump chain tends to infinity as $\lambda_2 \to \lambda_1$, then the lump chain will degenerate into a individual lump wave. The degeneration process can be observed in Fig. 2.

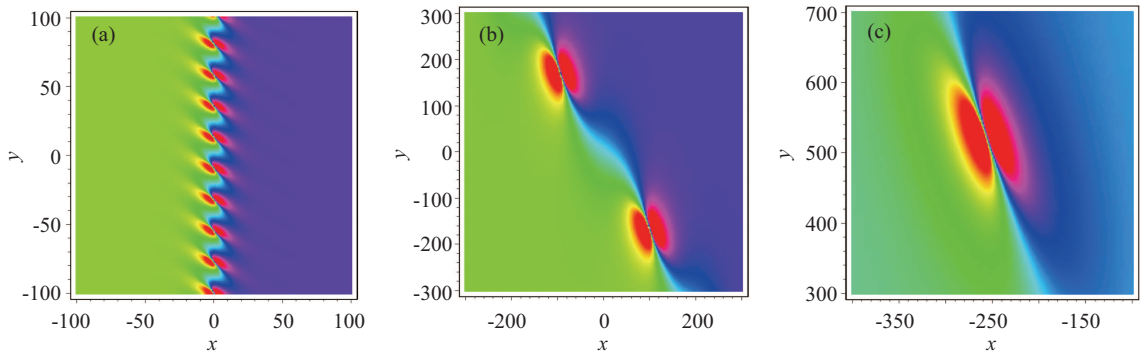


Fig. 2. The degeneration of the lump chain with $s = 1$ and $t = 0$. (a) $\lambda_1 = 1/2+\mathrm{i}/3$, $\lambda_2 = 1/3+\mathrm{i}/2$, (b) $\lambda_1 = 1/5+\mathrm{i}/6$, $\lambda_2 = 1/6+\mathrm{i}/7$, (c) $\lambda_1 = 1/9+\mathrm{i}/8$, $\lambda_2 = 1/10+\mathrm{i}/9$.

3.2. Lump chains with $M = 1$ and $N = 3$

In this section, we focus on the solutions of rank $M = 1$ and order $N = 3$. This kind of solution consists of three lump chains meeting at a triple point, which contains some degenerate configurations as the eigenvalues are different (see Fig. 3(a)). The phenomenon of the branched lump chain can be explained as the resonant interactions of breathers. As we can observe in Fig. 3(c), the three lump chain solutions are supported on the common boundaries of three regions Δ_1, Δ_2, and Δ_3. The boundary lies on the lines $F_n = F_m$ $(n,m = 1,2,3)$, respectively. The normal vectors of these lines can be given as $\boldsymbol{U}_{nm} = (\alpha_n - \alpha_m, 2\alpha_n\beta_n - 2\alpha_m\beta_m)$. The three normal vectors satisfy the condition $\boldsymbol{U}_{13} = \boldsymbol{U}_{12} + \boldsymbol{U}_{23}$, which also verifies why the three boundary lines cross to one point. The three normal vectors have the relationship that either collinear or pairwise linearly independent, which are determined by the formula $\Theta_{123} = A_{12}B_{13} - A_{13}B_{12} = (\alpha_1 - \alpha_2)(2\alpha_1\beta_1 - 2\alpha_3\beta_3) - (\alpha_1 - \alpha_3)(2\alpha_1\beta_1 - 2\alpha_2\beta_2)$. In general, the eigenvalues λ_1, λ_2, and λ_3 make Θ_{123} not zero and no two of the three vector $\boldsymbol{U}_{nm}$ are collinear. The three regions Δ_1, Δ_2, and Δ_3 form three sectors with common vertex in the (x,y)-plane. Three boundary lines $F_n = F_m$ $(n,m = 1,2,3)$ intersect at the triple point under the condition $F_1 = F_2 = F_3$. The lump chain from any branch is exponentially close to the lump chain of the order $N = 2$ presented by Eq. (13). As shown in Fig. 3(b), the $[1,2]$-lump chain lies on the ray $\Delta_1 \cap \Delta_2$, *i.e.*, $F_1 = F_2$. Along this ray one has $F_1 = F_2 \geq F_3$. It is a fact that there a constant $c > 0$ to make all the point on this ray satisfy the conclusion $F_1 - F_3 = F_2 - F_3 \geq cl$, where l is the distance to the triple point. When $N = 3$, the τ-function (11) can be reduced to

$$\begin{aligned}\tau(x,y,t,s) = {} & \mathrm{e}^{2F_1} + \mathrm{e}^{2F_2} + \mathrm{e}^{2F_3} + 4\theta_{12}\,\mathrm{e}^{F_1+F_2}\cos(G_1 - G_2 - \delta_{12}) \\ & + 4\theta_{13}\,\mathrm{e}^{F_1+F_3}\cos(G_1 - G_3 - \delta_{13}) + 4\theta_{23}\,\mathrm{e}^{F_2+F_3}\cos(G_2 - G_3 - \delta_{23}),\end{aligned} \tag{14}$$

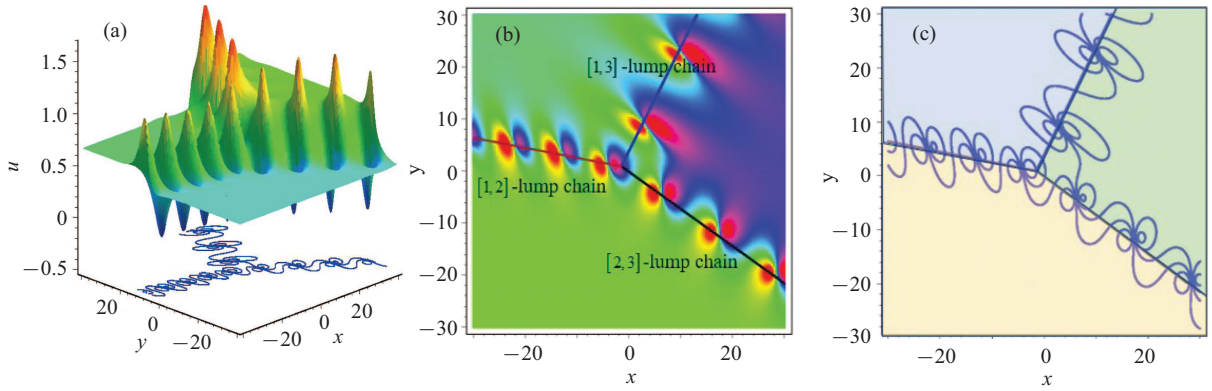


Fig. 3. Three lump chains when $M = 1$, $N = 3$, and the eigenvalues are chosen as $\lambda_1 = 1/3+\mathrm{i}/2$, $\lambda_2 = 1/4-\mathrm{i}/5$, $\lambda_3 = 1/2+\mathrm{i}/4$. (a) Three lump chains $u(x,y,t = 0,s = 1)$, (b) distribution diagram of lump chains, (c) Δ_1, Δ_2, and Δ_3 form a partition of the (x,y)-plane.

Factoring out the common term $\mathrm{e}^{F_1+F_2}$, the τ-function (14) is changed into

$$\begin{aligned}\tau(x,y,t,s) = {} & \mathrm{e}^{F_1+F_2}[\cosh(F_1 - F_2) + 2\theta_{12}\cos(G_1 - G_2 - \delta_{12}) + \frac{1}{2}\mathrm{e}^{2F_3-F_1-F_2} \\ & + 2\theta_{13}\,\mathrm{e}^{F_3-F_2}\cos(G_1 - G_3 - \delta_{13}) + 2\theta_{23}\,\mathrm{e}^{F_3-F_1}\cos(G_2 - G_3 - \delta_{23})],\end{aligned}$$

which has the equivalent form $\tau(x,y,t,s) = \mathrm{e}^{F_1+F_2}\left[\cosh(F_1 - F_2) + 2\theta_{12}\cos(G_1 - G_2 - \delta_{12}) + \tilde{h}\right]$,

where $|\tilde{h}| \leq C_1 \mathrm{e}^{-cl}$ along the ray $\Delta_1 \cap \Delta_2$. Thus we can conclude that the three lump chains are exponentially close to the lump chain (13) of the case $N = 2$ along this ray. We can see from Fig. 3(b) the solution with τ-function (11) and $N = 3$ consists of three lump chains having a common intersection when $\Theta_{123} \neq 0$. Each branch of the lump chains lies on the ray determined by $F_n = F_m$, which is called $[n,m]$-chain. Figure 3(b) shows that the lump chains $[1,2]$ and $[2,3]$ fuse together to create a new chain $[1,3]$. Conversely, the individual lump of the $[1,3]$-lump chain at the triple point splits into two lump chains. It is notable that the relative phases $\tilde{E}_{12} = \mathrm{Im}(\eta_n - \eta_m) = l_n - l_m$ have an influence on the position of the triple point, which can be observed in Fig. 4.

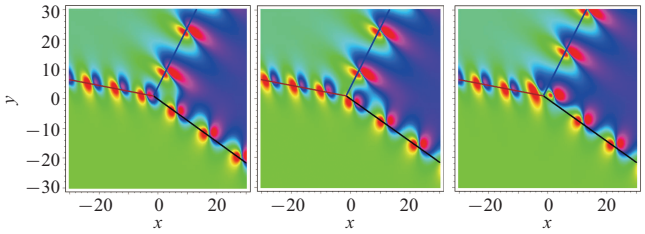


Fig. 4. Three lump chains when $M = 1$, $N = 3$ and the eigenvalues are chosen as $\lambda_1 = 1/3+\mathrm{i}/2$, $\lambda_2 = 1/4-\mathrm{i}/5$, $\lambda_3 = 1/2+\mathrm{i}/4$. (a) $\tilde{E}_{12} = 0$ and $\tilde{E}_{13} = 0$, (b) $\tilde{E}_{12} = \pi$ and $\tilde{E}_{13} = 0$, (c) $\tilde{E}_{12} = 0$ and $\tilde{E}_{13} = \pi$.

If the condition $\Theta_{123} = 0$ is satisfied, the three vectors $\boldsymbol{U}_{13}$, $\boldsymbol{U}_{12}$, and $\boldsymbol{U}_{23}$ are collinear, which leads to the two possible cases of the lump chains. (i) All the three regions Δ_1, Δ_2, and Δ_3 are nonempty, where Δ_1 and Δ_3 are half-planes. At the same time, the region λ_2 is a band shaped area of limited width. In this situation, the solution consists of two parallel lump chains, *i.e.*, $[1,2]$-lump chain and $[2,3]$-lump chain setting on the lines $\Delta_1 \cap \Delta_2$ and $\Delta_2 \cap \Delta_3$, respectively. This phenomenon can be seen in Figs. 5(a)–5(c). (ii) The region Δ_2 may be empty, so that $F_2 \leq \max(F_1, F_3)$ on the whole (x,y)-plane. The solution is supported along the line $F_1 = F_3$ and it is a simple $[1,3]$-lump chain, which can be observed in Fig. 5(d).

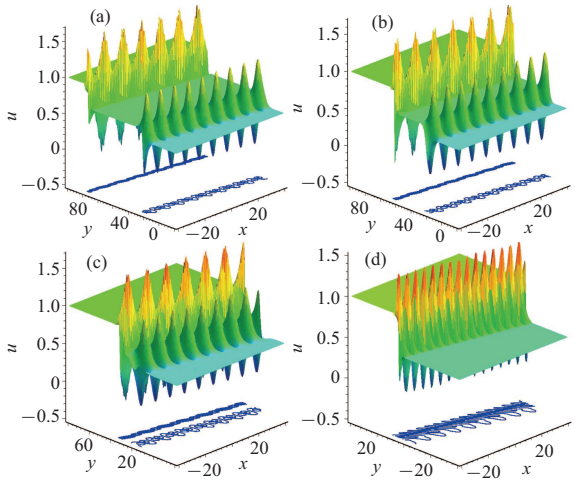


Fig. 5. The evolution of the lump chains when $M = 1$, $N = 3$ and the eigenvalues are chosen as $\lambda_1 = 1/3+\mathrm{i}/2$, $\lambda_2 = 1/4-\mathrm{i}/5$, $\lambda_3 = 1/2+6\mathrm{i}/5$, $s = 20$.

Combining conditions $A_{12}C_{13} - A_{13}C_{12} = 0$ and $\Theta_{123} = 0$ to the τ-function (14), we can obtain the solution consisting of two parallel lump chains with equal velocity. Depending on the values of the phases, the middle region Δ_2 either exists or is empty for all t. When Δ_2 is empty, the two parallel lump chains merge into one lump chain. The structure of the two parallel lump chains with equal velocity are similar to the breather molecules presented by Lou *et al.*[53–55] Thus we call this type of solution a lump chain molecule. The evolutionary behaviors of the lump chain molecule can be observed in Fig. 6. If the distance between two lump chains of the molecule is zero, the three lines $F_n = F_m$ are the same, then the lump chain molecule is reduced to a quasi-periodic lump chain, which can be seen in Fig. 7.

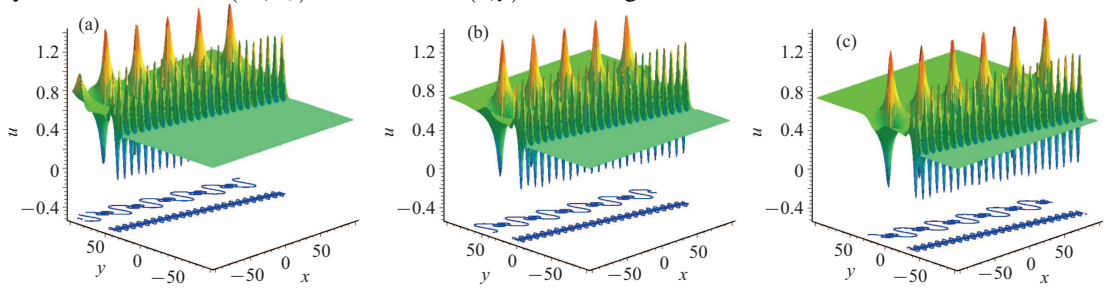


Fig. 6. Lump chain molecule determined by the τ-function (14) with $\lambda_1 = 1/3+\mathrm{i}/5$, $\lambda_2 = 1/4-\mathrm{i}/2$, $\lambda_3 = 0.367+0.393\mathrm{i}$, and $s = 30$.

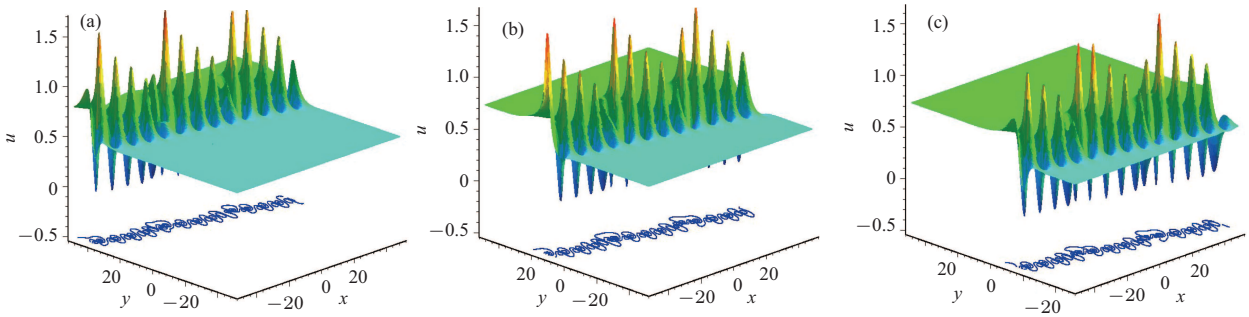


Fig. 7. Quasi-periodic lump chain determined by the τ-function (14) with $\lambda_1 = 1/3+\mathrm{i}/5$, $\lambda_2 = 1/4-\mathrm{i}/2$, $\lambda_3 = 0.367+0.393\mathrm{i}$, and $s = 0$.

3.3. Lump chains with $M = 1$ and $N \geq 4$

This section focuses on discussing the order $N \geq 4$, which is determined by the multiple eigenvalues λ_n. As the discussion in Subsection 3.1, every linear function F_n gives a polygonal partition Δ_n [Eq. (12)]. The boundaries $F_n = F_m$ determine sectors or polygonal regions evolving linearly with time, which may appear and disappear. On the boundary lines $\Delta_n \cap \Delta_m$, one has $F_n = F_m \geq F_j\,(j \neq n,m)$, then the every branch of the multiple lump chains can be approximated with exponential accuracy by the τ-function (11) of the case $N = 2$. Thus, on the every ray $\Delta_n \cap \Delta_m$, there is an $[n,m]$-lump chain. The multiple lump chains joint or split in the position of some independent lumps, meanwhile, the every lumps at intersections are preserved. The fluxes of lump chains through intersections satisfy the local conservation laws.

Figure 8 is plotted to show the H-type lump chains consisting of two triple points, where a lump chain bridge is connected between the two points. The lump chain bridge shrinks to a point when $t = 0$. With time t increasing, the lump chain bridge changes from the previous vertical direction to the horizontal direction, which can be observed in Figs. 8(a) and 8(c).

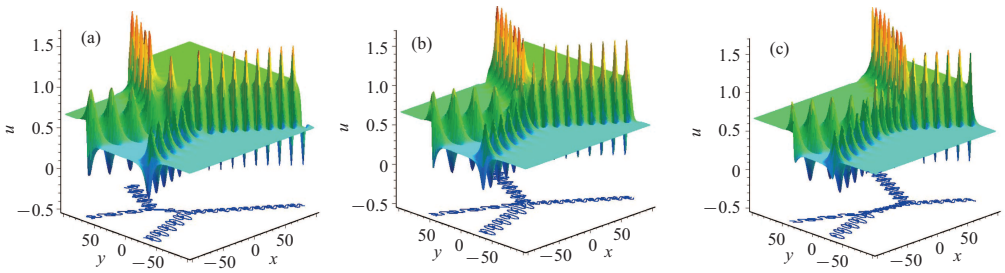


Fig. 8. The H-type lump chains when $M = 1$, $N = 4$, and the eigenvalues are chosen as $\lambda_1 = 1/3 + \mathrm{i}/2$, $\lambda_2 = 1/4 - \mathrm{i}/5$, $\lambda_3 = 1/2 + \mathrm{i}/4$, $\lambda_4 = 1/5 + \mathrm{i}/7$. (a) H-type lump chains $u\,(x,y,t = -20,s = 1)$, (b) H-type lump chains $u\,(x,y,t = 0,s = 1)$, (c) H-type lump chains $u\,(x,y,t = 20,s = 1)$.

3.4. Lump chains when the rank $M \geq 2$

The lump chain solution of the BKP equation with depth $P = 0$ and rank $M \geq 2$ is similar to the case of $M = 1$. The τ-function (3) also consists of two types of terms, *i.e.*, purely exponential function and mixed terms combining exponential function and trigonometric function. For a given moment t and a fixed parameter s, the (x,y) is divided into finite polygons. The τ-function has a dominant exponential term e^{2F_n} which produces an exponentially small solution inside of these regions. The decomposition of the regions evolves linearly with time, and some polygons may appear or disappear. The boundaries of the partitioned regions support the lump chains. For a intersection of boundaries, the flux of the arriving lump chains is equal to the flux of leaving lump chains. Figure 9 is presented to show the structure of the multiple lump chains with rank $M = 2$. The middle polygon lies vertical as t tends to negative values. All the lump chains gather together to one common point which can be observed in Fig. 9(b). Then the middle polygon gradually change to horizontal direction as time t tends to positive value. If time t is fixed, the auxiliary variable s plays an opposite effect on the structure for the middle polygon. The polygon changes from horizontal direction to vertical direction with the increase of s (see Fig. 10).

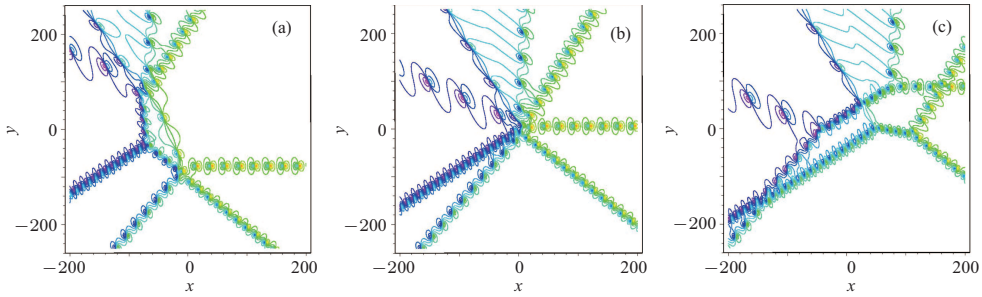


Fig. 9. The contour map of the lump chains when $M = 2$, $N = 4$, and the eigenvalues are chosen as $\lambda_{11} = 1/3 + \mathrm{i}/7$, $\lambda_{12} = 1/3 - \mathrm{i}/9$, $\lambda_{13} = 1/5 + \mathrm{i}/4$, $\lambda_{14} = 1/6 + \mathrm{i}/8$, $\lambda_{21} = 3/7 + \mathrm{i}/8$, $\lambda_{22} = 1/4 - \mathrm{i}/7$, $\lambda_{23} = 1/8 + \mathrm{i}/3$, $\lambda_{24} = 3/10 + 2\mathrm{i}/7$. (a) Lump chains $u\,(x,y,t = -200,s = 1)$, (b) lump chains $u\,(x,y,t = 0,s = 1)$, (c) lump chains $u\,(x,y,t = 200,s = 1)$.

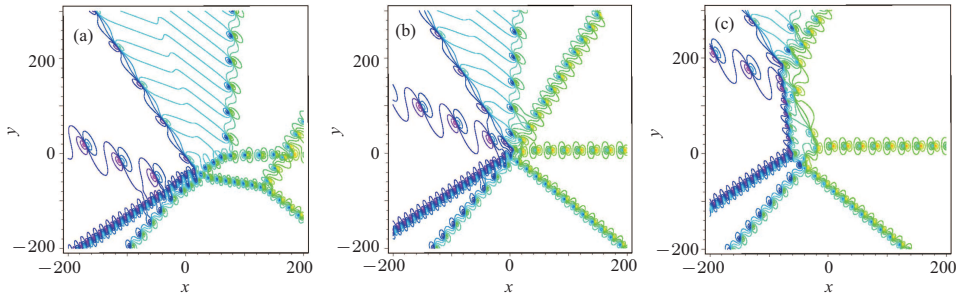


Fig. 10. Evolution of lump chains with the change of parameter s with the eigenvalues are given in Fig. 9. (a) Lump chains $u\,(x,y,t = 1,s = -150)$, (b) lump chains $u\,(x,y,t = 1,s = 0)$, (c) lump chains $u\,(x,y,t = 1,s = 150)$.

4. Interaction solutions between lump chains and kink-solitons

In this section, we mainly consider the interaction between the lump chains and kink-solitons of the BKP Eq. (1). A simple solution with depth $P=0$ shall be discussed. The τ-function of such a solution is near to the form of

$$\tau(x,y,t,s)=1+\sum_{n=1}^{N}\mathrm{e}^{2F_n}+\sum_{n=1}^{N-1}\sum_{m=n+1}^{N}4\theta_{nm}\mathrm{e}^{F_n+F_m}\cos(G_n-G_m-\delta_{nm}). \quad (15)$$

In before analysis, the (x,y)-plane is divided into some polygonal regions $\Delta_1,\ldots,\Delta_n$, where one of the terms e^{2F_n} in Eq. (15) is dominant. Sine the constant term 1 is added to the τ-function (15), a new region will be created as Δ_0. When $N=2$ the τ-function is reduced to

$$\tau(x,y,t,s)=1+\mathrm{e}^{2F_1}+\mathrm{e}^{2F_2}+4\theta_{12}\mathrm{e}^{F_1+F_2}\cos(G_1-G_2-\delta_{12}), \quad (16)$$

then the (x,y)-plane is partitioned into three polygonal regions Δ_0, Δ_1, and Δ_2 (see Fig. 11(b)). Inside of the region Δ_0 the τ-function is approximately constant, therefore the solution u is exponentially small. At the boundary of this region, *i.e.*, $\Delta_0\cap\Delta_1$, and $\Delta_0\cap\Delta_2$, the term 1 and one of e^{2F_1} and e^{2F_2} are two dominant terms in the τ-function (16). So along the boundary of the region where 1 dominates, there exists the kink-soliton, which can be observed in Fig. 11(a). At the same time, $\mathrm{e}^{F_1+F_2}$ is a dominant term in the τ-function (16) along the ray $\Delta_1\cap\Delta_2$. Therefore, a lump chain lies on the this ray. Figure 12 is plotted to show the evolutionary of the interaction between three kink-solitons and three lump chains. Along the boundaries of the dominant region Δ_0, there is a structure in which three solitons are connected, and one of which serves as a bridge. At the connection point of the solitons, two lump chain are split respectively. Then the lump chains and solitons form a structure of the capital letter X on the (x,y)-plane when $t=0$, and the bridging soliton disappears. With time goes on, the interaction solution consists of two kink-solitons and three lump chains, where a lump chain bridge connects two triple points.

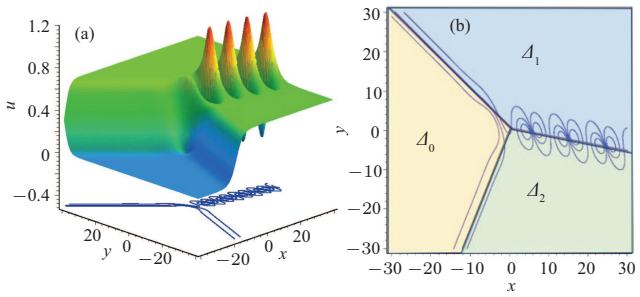


Fig. 11. The interaction solution between two kink-solitons and a lump chain as $M=1$, $N=3$ and the eigenvalues are chosen as $\lambda_1=1/3+\mathrm{i}/2$, $\lambda_2=1/4-\mathrm{i}/5$. (a) 3D stereogram of the solution $u(x,y,t=0,s=1)$, (b) contour map corresponding to panel (a) and the distribution of dominant domains.

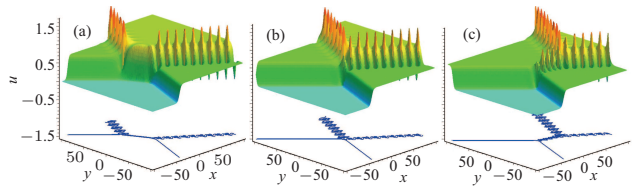


Fig. 12. The interaction solution between three kink-solitons and three lump chains a $M=1$, $N=3$, and the eigenvalues are chosen as $\lambda_1=1/3+\mathrm{i}/2$, $\lambda_2=1/4-\mathrm{i}/5$, $\lambda_3=1/2+\mathrm{i}/4$.

5. Hybrid solutions consisting of lump chains and lumps

By considering the general form of the τ-function in the solution (3), we know that if $c_{jk}=0$ and each φ_j is a polynomial multiple a exponential function $\mathrm{e}^{\sigma(x,y,t,s,\lambda_j)}$, the τ-function is a rational function and the corresponding solution is localized in the plane (x,y). Especially, if all the eigenfunctions λ_j are different, the nonlinear phenomenon of interaction between multiple lump molecules can be presented. The polynomial terms play a minor impact on the τ-function than the exponentials when x and y are large enough. Therefore, it is meaningful to investigate the φ_j function consisting of purely exponentials, which corresponds to the case of depth $P=0$ discussed in Section 3. The solution has a structure of lump chains in this case. However, the polynomials of the φ_j-function (8) cannot be ignored in the finite part of the (x,y)-plane. The polynomial terms produce individual lumps in the solution actually. Thus the solution possesses the structure of lump chains interacting with several individual lumps. The lumps may be emitted or absorbed by the lump chains during the interactions. In this section, we attempt to investigate some classifications of such solutions. Taking rank $M=1$, order $N=2$ and depth $P=1$ in formula (8), the φ-function can be expanded as

$$\varphi(x,y,t,s)=C_{10}\rho_0\mathrm{e}^{\sigma(x,y,t,\lambda_1)}+C_{20}\rho_0\mathrm{e}^{\sigma(x,y,t,\lambda_2)}+C_{11}\rho_1\mathrm{e}^{\sigma(x,y,t,\lambda_1)}+C_{21}\rho_1\mathrm{e}^{\sigma(x,y,t,\lambda_2)}, \quad (17)$$

where its conjugate function can be given as

$$\bar{\varphi}(x,y,t,s)=C_{10}\bar{\rho}_0\mathrm{e}^{\bar{\sigma}(x,y,t,\lambda_1)}+C_{20}\bar{\rho}_0\mathrm{e}^{\bar{\sigma}(x,y,t,\lambda_2)}+C_{11}\bar{\rho}_1\mathrm{e}^{\bar{\sigma}(x,y,t,\lambda_1)}+C_{21}\bar{\rho}_1\mathrm{e}^{\bar{\sigma}(x,y,t,\lambda_2)}. \quad (18)$$

Substituting them into solution (3) with $c_{jk}=0$, one can obtain the hybrid solutions consisting of the individual lumps and the single lump chain. If the coefficient $C_{20}=0$ and other coefficients are nonzero (without losing generality, they were all let to be 1), the solution presents the structure of a lump chain absorbing an individual lump with the evolution of the auxiliary variable s.

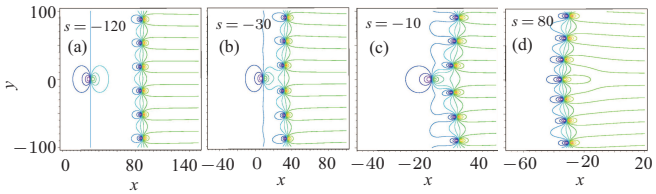


Fig. 13. An individual lump is absorbed by a lump chain with rank $M=1$, $N=2$, and depth $P=1$, and $\lambda_{11}=1/2$, $\lambda_{12}=1/4$, $t=1$.

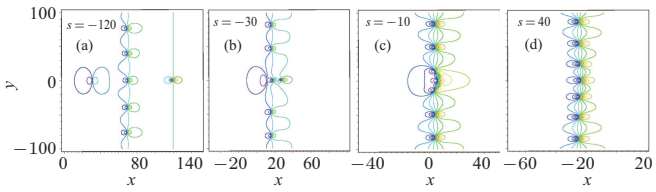


Fig. 14. The interaction between two lump chains and two lumps with rank $M=1$, $N=2$, and depth $P=1$, and $\lambda_{11}=1/2$, $\lambda_{12}=1/4$, $t=1$.

As shown in Fig. 13, the left single lump is gradually absorbed by the right lump chain, which can be regarded as a phenomenon of the rogue wave controlled by the parameters. If all the coefficients C_{np} are nonzero, the solution consists of two lumps and a lump chain as s tends to be a negative larger value, which is shown in Fig. 14(a). Then both of the two lumps gradually integrate into the lump chain as a whole with the lumps in the original lump chain (as shown in Figs. 14(b)–14(d)).

If we take rank $M=2$, order $N=2$, and depth $P=1$ in formula (8), the φ-function has the following forms:

$$\begin{aligned}\varphi_1 &= C_{110}\rho_0(x,y,t,s,\lambda_{11})\,\mathrm{e}^{\sigma(x,y,t,s,\lambda_{11})}\\ &\quad + C_{111}\rho_1(x,y,t,s,\lambda_{11})\,\mathrm{e}^{\sigma(x,y,t,s,\lambda_{11})}\\ &\quad + C_{120}\rho_0(x,y,t,s,\lambda_{12})\,\mathrm{e}^{\sigma(x,y,t,s,\lambda_{12})}\\ &\quad + C_{121}\rho_1(x,y,t,s,\lambda_{12})\,\mathrm{e}^{\sigma(x,y,t,s,\lambda_{12})},\\ \varphi_2 &= C_{210}\rho_0(x,y,t,s,\lambda_{21})\,\mathrm{e}^{\sigma(x,y,t,s,\lambda_{21})}\\ &\quad + C_{211}\rho_1(x,y,t,s,\lambda_{21})\,\mathrm{e}^{\sigma(x,y,t,s,\lambda_{21})}\\ &\quad + C_{220}\rho_0(x,y,t,s,\lambda_{22})\,\mathrm{e}^{\sigma(x,y,t,s,\lambda_{22})}\\ &\quad + C_{221}\rho_1(x,y,t,s,\lambda_{22})\,\mathrm{e}^{\sigma(x,y,t,s,\lambda_{22})}.\end{aligned}$$

Then the τ-function can be written as

$$\tau(x,y,t,s)=\begin{vmatrix}\displaystyle\int_{-\infty}^{x}\varphi_1\bar{\varphi}_1\,\mathrm{d}x' & \displaystyle\int_{-\infty}^{x}\varphi_1\bar{\varphi}_2\,\mathrm{d}x'\\ \displaystyle\int_{-\infty}^{x}\varphi_2\bar{\varphi}_1\,\mathrm{d}x' & \displaystyle\int_{-\infty}^{x}\varphi_2\bar{\varphi}_2\,\mathrm{d}x'\end{vmatrix},$$

which leads to a solution consisting of two lumps and two parallel lump chains as s is a negative large value as shown in Fig. 15(a).

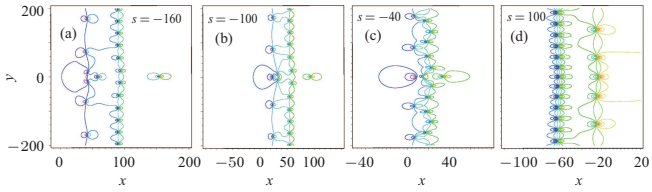


Fig. 15. The interaction between two lump chains and two lumps with rank $M=2$, $N=2$, and depth $P=1$, and $\lambda_{11}=1/2$, $\lambda_{12}=1/4$, $\lambda_{21}=1/3$, $\lambda_{22}=1/5$, $t=1$.

With s increasing, the two lump chains close to each other and two lump waves are located on both sides (see Figs. 15(b) and 15(c)). If s is a positive large value, the solution consists of the two parallel lump chains, *i.e.*, the two lumps are absorbed by the lump chains as increase of s.

For investigating the higher depth interaction solutions, we choose rank $M=2$, order $N=2$, and depth $P=2$ in formula (8), then the φ-function can be expanded as

$$\begin{aligned}\tilde{\varphi}_1 &= C_{110}\rho_0(x,y,t,s,\lambda_{11})\,\mathrm{e}^{\sigma(x,y,t,s,\lambda_{11})}+C_{111}\rho_1(x,y,t,s,\lambda_{11})\,\mathrm{e}^{\sigma(x,y,t,s,\lambda_{11})}\\ &\quad + C_{112}\rho_2(x,y,t,s,\lambda_{11})\,\mathrm{e}^{\sigma(x,y,t,s,\lambda_{11})}+C_{120}\rho_0(x,y,t,s,\lambda_{12})\,\mathrm{e}^{\sigma(x,y,t,s,\lambda_{12})}\\ &\quad + C_{121}\rho_1(x,y,t,s,\lambda_{12})\,\mathrm{e}^{\sigma(x,y,t,s,\lambda_{12})}+C_{122}\rho_2(x,y,t,s,\lambda_{12})\,\mathrm{e}^{\sigma(x,y,t,s,\lambda_{12})},\\ \tilde{\varphi}_2 &= C_{210}\rho_0(x,y,t,s,\lambda_{21})\,\mathrm{e}^{\sigma(x,y,t,s,\lambda_{21})}+C_{211}\rho_1(x,y,t,s,\lambda_{21})\,\mathrm{e}^{\sigma(x,y,t,s,\lambda_{21})}\\ &\quad + C_{212}\rho_2(x,y,t,s,\lambda_{21})\,\mathrm{e}^{\sigma(x,y,t,s,\lambda_{21})}+C_{220}\rho_0(x,y,t,s,\lambda_{22})\,\mathrm{e}^{\sigma(x,y,t,s,\lambda_{22})}\\ &\quad + C_{221}\rho_1(x,y,t,s,\lambda_{22})\,\mathrm{e}^{\sigma(x,y,t,s,\lambda_{22})}+C_{222}\rho_2(x,y,t,s,\lambda_{22})\,\mathrm{e}^{\sigma(x,y,t,s,\lambda_{22})}.\end{aligned}$$

Utilizing above pair of functions, the τ-function can be rewritten as

$$\tau(x,y,t,s)=\begin{vmatrix}\displaystyle\int_{-\infty}^{x}\tilde{\varphi}_1\bar{\tilde{\varphi}}_1\mathrm{d}x' & \displaystyle\int_{-\infty}^{x}\tilde{\varphi}_1\bar{\tilde{\varphi}}_2\mathrm{d}x'\\ \displaystyle\int_{-\infty}^{x}\tilde{\varphi}_2\bar{\tilde{\varphi}}_1\mathrm{d}x' & \displaystyle\int_{-\infty}^{x}\tilde{\varphi}_2\bar{\tilde{\varphi}}_2\mathrm{d}x'\end{vmatrix}.$$

By substituting the above expression into the variable transformation $u=(\ln\tau)_x$, the hybrid solutions consisting of two lump chains and more individual lumps are obtained. As shown in Fig. 16, the depth P determines the number of the lump waves. There exist seven lumps lying on both sides of the two

lump chains as s is equal to -160. With s increasing, the right lumps form a structure of a triangle and the left three lumps are gradually absorbed by the lump chain on the left side. Figures 16(c) and 16(d) show that the lumps are finally absorbed by the lump chains with the increase of the parameter s.

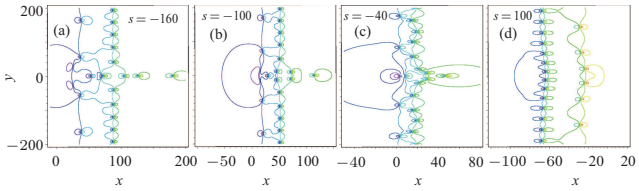


Fig. 16. The interaction between two lump chains and seven lumps with rank $M = 2$, $N = 2$, and depth $P = 2$, eigenvalues are selected as the same as Fig. 15 and $t = 1$.

6. Conclusions

In this paper, we mainly pay our attention to investigating the lump chains and interaction solutions of the BKP equation describing the propagation dynamics of the nonlinear waves appearing in physics, biology, and electrical networks. A τ-function in the form of Grammian (3) is utilized to start our discussion. Thus a family of the lump chain solutions by means of the general τ-function (11) are obtained. The lump chains consist of an infinite of equally spaced individual lumps. Every single lump chain has two characteristic lines, and one of which determines the direction vector and the other plays a role in controlling the twist direction of the individual lump among the lump chains. Each of branch of the lump chains lies on the ray determined by the dominant regions $\Delta_n \cap \Delta_m$, where Δ_n is given by formula (12). The multiple lump chains fuse or scatter at some intersections. All lumps at intersections are preserved, *i.e.*, the fluxes of lump chains through intersections satisfy the local conservation laws. In order to extend the types of the lump chains, some general solutions consisting of parallel, superimposed, and molecular lump chains are presented. Furthermore, the H-type lump chains (as shown in Fig. 8) and the complex lump chains with rank $M = 2$ (as shown in Figs. 9 and 10) are obtained. The crossing regions among the multiple lump chains may appear or disappear, and the middle polygon rotates with time t and the auxiliary parameter s.

It is possible to consider the interaction solutions between the lump chains and the kink-solutions by adding a constant term 1 in the τ-function (15). Along the boundaries determined by the dominant regions of the constant term, there exist the kink-solitons (as shown in Figs. 11 and 12). By considering the higher order N, we can investigate more complex interaction waves between lump chains and solitons. In order to investigate a new kind of interaction solutions controlled by the parameter s, we consider the eigenfunctions (8) to the following three cases:

(i) rank $M = 1$, order $N = 2$ and depth $P = 1$;

(ii) rank $M = 2$, order $N = 2$ and depth $P = 1$;

(iii) rank $M = 2$, order $N = 2$ and depth $P = 2$.

These kinds of solutions can be regarded as new types of "rogue waves" describing the phenomena of absorbing or emitting individual lumps for the lump chains.

A large family of lump chain, interaction, and rogue wave solutions obtained in this paper are helpful to further analyze the scientific problems described by BKP Eq. (1). Studying the detailed classification of the solutions from the perspective of τ-function in the form of Grammian is an interesting and difficult topic. We will continue to conduct our investigations in this field.

Acknowledgments

Project supported by the National Natural Science Foundation of China (Grant No. 12101572) and the Research Project Supported by Shanxi Scholarship Council of China (Grant No. 2020-105).

References

[1] Chang J H 2018 *Theor. Math. Phys.* **195** 676
[2] Ma W X 2015 *Phys. Lett. A* **379** 1975
[3] Yuan P S, Qi J X, Li Z L and An H L 2021 *Chin. Phys. B* **30** 040503
[4] Zhang Z, Yang X Y, Li W T and Li B 2019 *Chin. Phys. B* **28** 110201
[5] Zhao Z L and He L C 2022 *Nonlinear Dyn.* **108** 555
[6] Zhao Z L and He L C 2022 *Commun. Theor. Phys.* **74** 105004
[7] Zhao Z L and He L C 2019 *Appl. Math. Lett.* **95** 114
[8] Manakov S V, Zakharov V E, Bordag L A, Its A R and Matveev V B 1977 *Phys. Lett. A* **63** 205
[9] Ablowitz M J and Satsuma J 1978 *J. Math. Phys.* **19** 2180
[10] Satsuma J and Ablowitz M J 1979 *J. Math. Phys.* **20** 1496
[11] Gorshkov K A, Pelinovsky D E and Stepanyants Y A 1993 *JETP* **104** 2704
[12] Pelinovsky D E and Stepanyants Y A 1993 *JETP Lett.* **57** 24
[13] Pelinovsky D 1994 *J. Math. Phys.* **35** 5820
[14] Pelinovsky D 1998 *J. Math. Phys.* **39** 5377
[15] Chakravarty S and Zowada M 2022 *J. Phys. A: Math. Theor.* **55** 215701
[16] Chakravarty S and Zowada M 2022 *J. Phys. A: Math. Theor.* **55** 195701
[17] Zhang Z, Li B, Wazwaz A M and Guo Q 2022 *Phys. Lett. A* **424** 127848
[18] Zhao Z L and He L C 2022 *Nonlinear Dyn.* **109** 1033
[19] Yang B and Yang J K 2022 *J. Nonlinear Sci.* **32** 52
[20] Zhang Z, Qi Z Q and Li B 2021 *Appl. Math. Lett.* **116** 107004
[21] Zhao Z L and He L C 2021 *Appl. Math. Lett.* **122** 107497
[22] He L C, Zhang J W and Zhao Z L 2021 *Nonlinear Dyn.* **106** 2515
[23] Rao J G, Chow K M, Mihalache D and He J S 2021 *Stud. Appl. Math.* **147** 1007
[24] Guo L J, Chabchoub A and He J S 2021 *Physica D* **426** 132990
[25] Rao J G, Kanna T, Mihalache D and He J S 2022 *Physica D* **439** 13
[26] Rao J G, Fokas A S and He J S 2021 *J. Nonlinear Sci.* **31** 67
[27] Li M, Fu H M and Wu C F 2020 *Stud. Appl. Math.* **145** 97
[28] Stepanyants Y A, Zakharov D V and Zakharov V E 2022 *Radiophys Quantum El.* **64** 665
[29] Lester C, Gelash A, Zakharov D and Zakharov V 2021 *Stud. Appl. Math.* **147** 1425
[30] Tajiri M and Murakami Y 1989 *J. Phys. Soc. Jpn.* **58** 3029
[31] Zaitsev A A 1983 *Sov. Phys. Dokl.* **28** 720

[32] Adamashvili G T and Kaup D J 2004 *Phys. Rev. E* **70** 066616
[33] Reigada R, Sancho J M, Iba? nes M and Tsironis G P 2001 *J. Phys. A: Math. Gen.* **34** 8465
[34] Zhang Z, Li B, Chen L C and Guo Q 2022 *Nonlinear Dyn.* **108** 4157
[35] Zhang Z, Li B, Chen L C, Guo Q and Stepanyants Y 2022 *Commun. Nonlinear Sci. Numer. Simul.* **112** 106555
[36] Bogoyavleskii O I 1990 *Lett. Nuovo Cimento Math. USSR. Izv.* **34** 245
[37] Calogero F 1975 *Lett. Nuovo Cimento* **14** 43
[38] Xie X Y, Tian B, Sun W R, Wang M and Wang Y P 2015 *Mod. Phys. Lett. B* **29** 1550192
[39] Estévez P G and Hernáez G A 2000 *J. Phys. A: Math. Gen.* **33** 2131
[40] Lü Z S and Zhang H Q 2003 *Chaos Solitons Fractals* **17** 669
[41] Wang C J and Fang H 2017 *Comput. Math. Appl.* **74** 3296
[42] Zhao Z L, Yue J and He L C 2022 *Appl. Math. Lett.* **133** 108294
[43] Yuan F, He J S and Chen Y 2021 *Chin. J. Phys.* **71** 190
[44] He L C, Zhang J W and Zhao Z L 2022 *Chinese J. Phys.* **79** 225
[45] Hirota R 2004 *The direct method in soliton theory* (Cambridge: Cambridge University Press)
[46] Wazwaz A M 2022 *Nonlinear Dyn.* **109** 1929
[47] Wazwaz A M 2020 *Phys. Lett. A* **384** 126787
[48] Wang C J and Fang H 2022 *Nonlinear Dyn.* **100** 583
[49] Chakravarty S and Kodama Y 2008 *J. Phys. A: Math. Theor.* **41** 275209
[50] Akhmediev N and Korneev V I 1986 *Theor. Math. Phys.* **69** 1089
[51] Kuznetsov E A 1977 *Sov. Phys. Dokl.* **22** 507
[52] Ma Y C 1979 *Stud. Appl. Math.* **60** 43
[53] Lou S Y 2020 *J. Phys. Commun.* **4** 041002
[54] Yan Z W and Lou S Y 2020 *Commun. Nonlinear Sci. Numer. Simul.* **91** 105425
[55] Zhang Z, Yang X Y and Li B 2020 *Nonlinear Dyn.* **100** 1551